1 Introduction

1.1 Objective : Improve the TFM Readout

Many different types of ultrasound scans exist, which are commonly used and accepted . Each method has its own detection limitations and when the industry introduces a new scan type, it will be to overcome intrinsic ultrasound physics issues. For example, dual crystal probes have been successfully used to address near-surface resolution issues and improve corrosion detection.

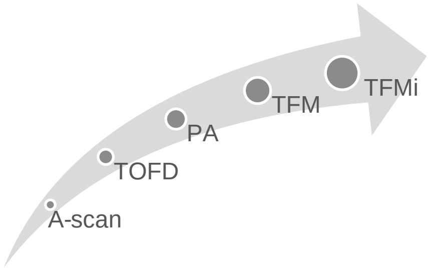

Figure 1: Evolution of the Ultrasound scan in the last decades

The most recent transition is the phased- array inspection to the Total Focusing Method (TFM) imaging type. TFM improves focusing resolution by introducing 64 element aperture size without the downside of a short depth of field usually associated with conventional PA methods . Therefore , in comparison with typical 16 to 64 element PA scans, we can now enhance the scan image by using two or more propagation modes , which provide additional multi -directional information .

To illustrate the evolution of ultrasound scan, here are all the common techniques over the same defect . From left to right, the conventional UT on a slag inclusion, a 15 MHz TOFD scan, a shear -wave sectorial - scan, a 2-skip “TT” TFM scan, and a multi shear mode TFM scan.

Conventional UT	TOFD scan

2-Skip PA Sectorial Scan	2-Skip TT Region of Interest - TFM (equivalent to TT and TTTT)
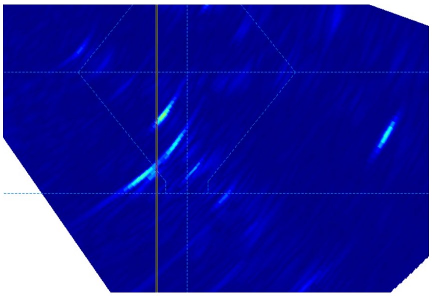	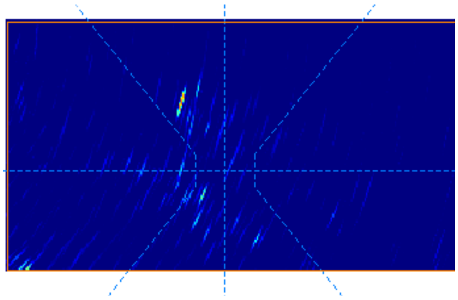
TT, TTT & TTTT TFMi™	
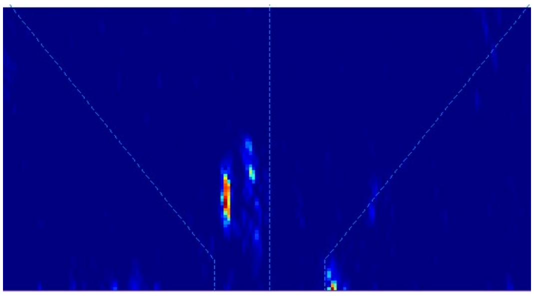	

Figure 2: Ultrasound Scan Evolution: A-scan->TOFD->PA->TFM->TFMi™

The first advantage of the TFMi method is its improved ease of interpretation. By removing the need for a multi skip representation, such as those that are present in, for instance, ordinary TT TFM or PA sectorial scans, the need for operator interpretation is reduced.

A second advantage is a reduced need for the operator to determine the proper mode to use for a particular flaw type. When the defect produces a combination of direct, indirect, and tip diffraction reflection patterns, an intermodal TFM analysis will provide a more complete image than an individual mode alone. It has been described in 2019 that using single-mode TFM does not meet the ASME welding requirements while the ISO stands with one specific propagation mode that solves classical weld inspection situations. Please refer to end note number 1 and 2 for that matter.

Usual TFM modes (LL, TT, TTTT, …) alone are liable to not meet the ASME welding requirements (section XI481.1.1) , as was demonstrated in a 2019 ASME standard reference article[1,2]. We develop herein a multi-mode technique to counter an uneven inter-mode sensitivity[3]. The consequence of using only one mode might lead to incomplete inspection coverage, for example.

In this paper, we will evaluate the intermodal scan performance in a usual context of weld inspection. Once the TFMi will be explained, the performance metrics of a TFMi scan will be exposed. We will show the geometry fidelity results that is a defect characterisation criterion, the amplitude metrics and dimensions performances that are quantitative metrics for defect evaluation.

1.2 TFM imagery to Intermode Evolution

Since the TFM frame is still strongly related to the propagation mode, for each separate mode, there are many mathematical combinations possible to obtain an Intermode image. During the post-recording step, the instrument could add the contributions of all or many modes. The image produced is then rendered on screen, just like any usual TFM scan.

In the past years, some researchers have developed offline intermodal techniques to improve flaw assessment. The purpose always remains similar: improve flaw size accuracy and enhance the fidelity of the flaw shape and orientation. There is a simple way namely it is pixel sum into the same frame[4]. There are also noise weight and modal image averaging that demonstrate useful sizing capability over large defects[5].

This study introduces the multiplicative intermode technique. Further applied in the rest of NDT, the study targets the flat weld inspections. The weld samples contain many kinds of artificial flaws so it would be possible to compare between TFMi™ scan and single-mode scans over crack, porosity and the lack of fusion.

2 The Intermode Parameters

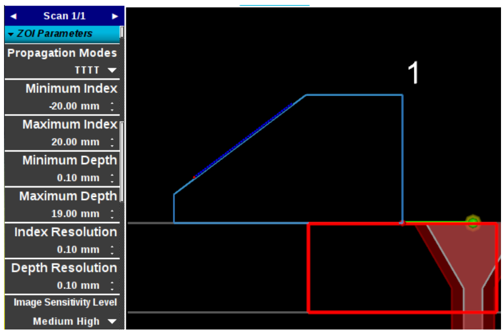

Sonatest's TFM Intermode solution generates standard "mono-modal" TFM frames which are then combined and rendered as a single scan image. The scan parameters of an Intermode scan remain the same as a TFM scan. The Intermode can be ranked from TT/TTTT up to TT/TTT/TTTT/5T. The region of interest (ROI) is defined by a rectangular box and the independent index and depth resolutions.

The propagation modes in the study are the same as presented and described in the document "ANNEX 1 V-1812-18 R1 FMC-TFM for weld testing – IIW" or the ASME appendix F, Ultrasonic Imaging Paths/Modes table[6]. Implementation

2.1 TFMi Image Processing

Given a set of same-coordinate TFM pixels P_1 to, P_n coming from TFM frames having different modes, the construction of a same-coordinate TFMi pixel P* is straightforward. Without loss of generality, we may suppose each Pi is within the range [0, 1]. Then, in order to construct P*, we simply take the products of the Pi, that is:

$$P^* = P_1 * P_2 * \ldots * P_n$$

This mode of combination will have a tendency to only show significant pixel amplitude in those places where the mode of every underlying TFM frame agrees, I.e. where all Pis are greater than 0 by a significant enough margin.

A concern may here be raised whether it would not be possible for one pixel of the product to be 0, while all other pixels should be 1, thus resulting in a final TFMi pixel P* of amplitude 0, in spite of the fact that all other pixels represented very strong signals. While this is a theoretical possibility, it does not represent a real risk in practice, as fundamental signal noise virtually always ensures that all pixel values will be greater than 0, be it by a very small margin.

Another concern is that since the underlying pixels were supposed to be contained within the range [0,1], it follows that P1*P2*…*Pn < Pi for all Pi except in those cases where P1 = P2 = … = Pn and Pi is either 0 or 1. Therefore, it would seem as though multiplication as described above has an attenuating effect on the resulting TFMi pixel. For instance, suppose a TFMi generated from three underlying TFM frames and suppose P1 = P2 = P3 = 0.8. Then P* = 0.8*0.8*0.8 = 0.512.

First, the full matrix capture (FMC) covers the necessary time of flight for all modes. For a 3-mode TFMi^{TM}, there will be 3 multiplied elementary pixels for a given pixel. In other words, a single-pixel sets all Tx-Rx element pairs, but each sample are then multiplied to generate the TFMi^{TM} image.

$$\begin{bmatrix} a & b \\ c & d \end{bmatrix}_{TT} * \begin{bmatrix} e & f \\ g & h \end{bmatrix}_{TTT} * \begin{bmatrix} i & j \\ k & l \end{bmatrix}_{TTTT} = \begin{bmatrix} aei & bfj \\ cgh & dhl \end{bmatrix}_{TT/TTT/TTTT}$$

Each sub-assembly pixel has a digital recording precision of 8 bits. That precision preserves the amplitude for all TFM scans. It is although post-processed at 16 bits. In the case of multiplied algorithms, all near zeros modes will not amplify the background noise but will reduce it.

It has been proven that a specific type of reflector does not provide the same amplitude response between the usual transverse TT and TT-TT modes. The modes that would likely require more gain are indirect modes (Odd number modes)[7]. For instance, the 5T mode is more susceptible than other modes to suffer from the effect of material attenuation as its usually represent a longer time of flight sound path. To address this issue, we have added an amplitude image correction. That increases the weight of the pixel samples above a specific threshold. The correction function works like this:

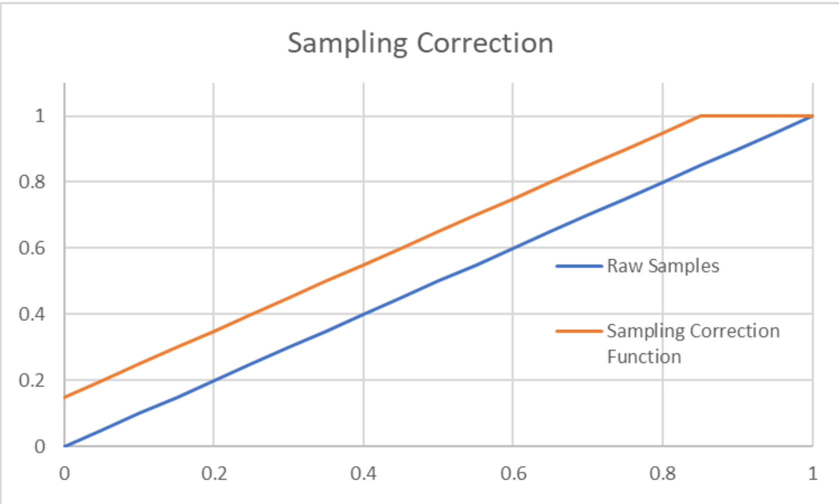

2.2 Proof of Concept

As a first demonstration, let's take 3 modes that will be merged in a TFMi™ frame. The PA setup consists of a 7.5 MHz probe with 0.6 mm of pitch and an active aperture of 44 elements. The array is attached to a 60-degree shear wave wedge. The individual modes are TT, TTT and TT-TT. They were simultaneously recorded at the same region of interest.

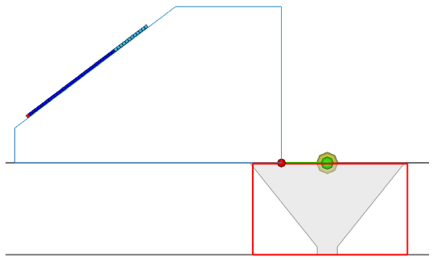	Thickness = 16 mm Wedge index offset = 8 mm ROI = -5 mm to 22 mm index axis Resolution = 0.1 mm x 0.1 mm Expected Flaw = Center line crack

Table 1: Processing TFM in a spreadsheet – 2 grades of colours

TT	TTT	TT-TT
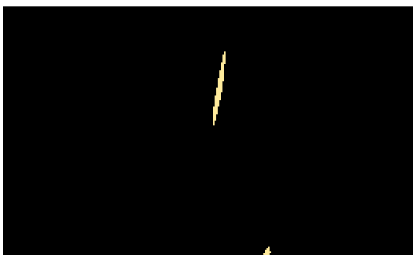	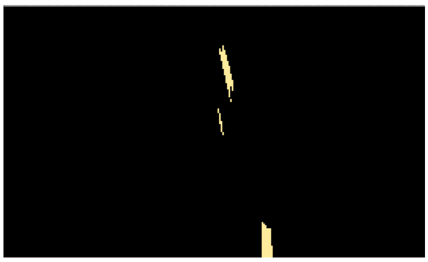	

TT+TTT+(TT-TT) TFMi™	TT*TTT*(TT-TT) TFMi™
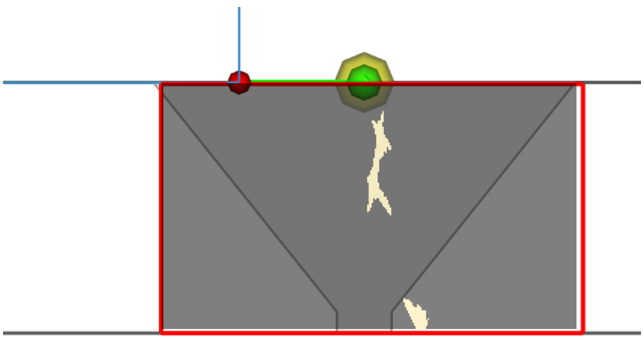	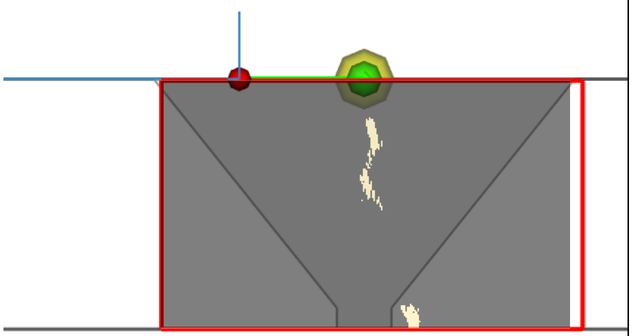

For this experience, the additive TFMi^{TM} keeps the beam characteristics underlying each sub-mode. This beam size contours the flaw ends because of its propagation and reflection direction.

On the other hand, the multiplicative TFM clears this beam-width effect because the high peak pixels dominate on screen. The multiplicative effect indeed increases the “presence” of a reflector when more than one mode is superimposed. When two modal echoes come from the same reflector, the multiplication does a coherence effect exactly where they overpass. As a result, the image content is mostly built by constructive multiplication of very close indications. The exact “beam” size function and the probe aperture impact is not quantified herein but it would deserve a study.

Regarding the background pixels, the baseline noise of the image is typically less than 5%. Therefore, this algorithm dilutes the noise contribution. Further in the real flaw analysis section, the signal-to-noise ratio results will be discussed.

2.2.1 Intermode on Real Flaws – Geometric Fidelity

There is an important benefit of having a precise and accurate non-destructive technique for defect classification purposes. In an image testing analysis, the aspect (or the shape/contour) of the echo and its location in the part will give evidence to categorize the defect.

The TFMi^{TM} view delivers a high-definition cross-section image of the weld. Its visual analysis is easier than the conventional PA/TFM with crescent-shaped echoes. Moreover, by using the weld overlay pointer lines, the user can effortlessly check the location and set the defect classification.
The outline of the defects is amplified by the contribution of TFM modes therefore the image is closer to real nature of the flaw.

The following results show all the defect types among the weld coupons.

Type of Defects	TFMi™ Mode	Weld Cross Section Image	Encoded side view (D-scan)
Lack of fusion in single V, surface breaking at root	TT/TTTT/5T	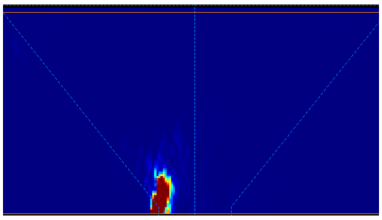	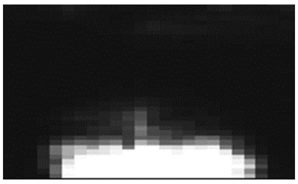
Root crack in single V, inner surface breaking	TT/TTT/TTTT	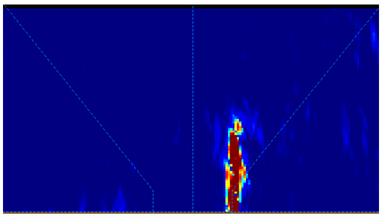	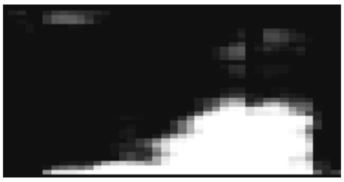
Lack of Fusion in single V, mid-wall area	TT/TTTT/5T	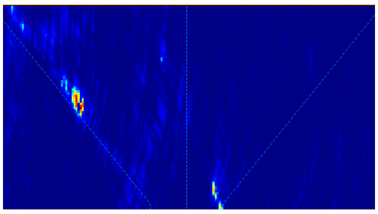	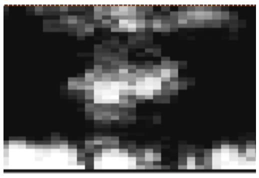
Porosity in single V, sub-surface	TT/TTT/TTTT	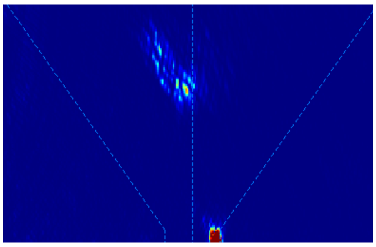	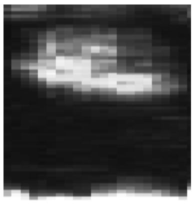
Centerline crack, sub surface	TT/TTT/TTTT	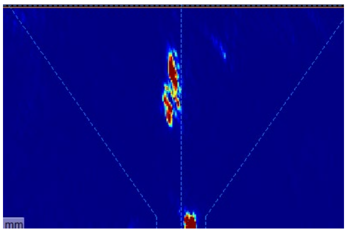	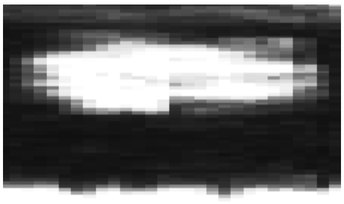
Slag inclusion in single V, under the weld crown area	TT/TTT/TTTT	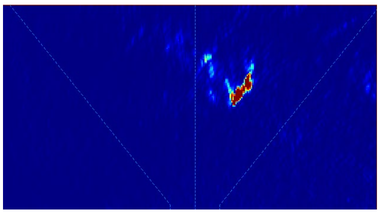	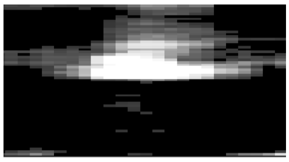
Toe Crack in single V	TT/TTTT/5T	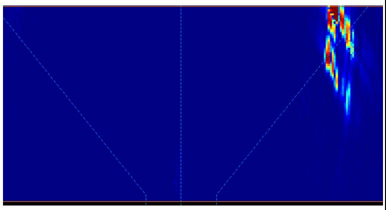	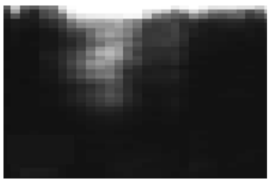

Table 2: Weld TFMi™ shots and its side view results

3 Quantitative Analysis over Weld Coupons

3.1 Sensitivity Analysis

The sensitivity level over the inspection specimen is an ongoing concern of ultrasonic NDT as inadequate sensitivity may result in the operator missing important flaw indications. To make sure there is no potential sensitivity loss over the TFM and TFMi, many flaw types have been recorded. The amplitude of each has been saved in a dB ratio. Among the 7 samples, each having 2 defects, 4 flaws were selected and the scanning gain was recorded for each single TFM mode and three different shear wave inter-modes. The thickness is 16 or 19 mm, the probe was a D1A 7.5MHz 0.6x12 mm and its active aperture was 32 elements.

TFM Mode(s)**	Scanning Gain (dB) Lack of fusion (LoF) mid wall area 3.8 mm - 2.5 from the surface	Scanning Gain (dB) LoF in V surface breaking at root 3.8 mm surf breaking	Scanning Gain (dB) Longitudinal crack in Single V (@ Flush Crown) 3.8 mm surf. breaking	Scanning Gain (dB) Center line Crack Sub surface 3.8 mm height
TT	39	32	N/A*	46
TTT	50	32.5	49.8	44
TTTT	30	29	47	47
5T	45	45	46	40
TT/TTT/TTTT	65	50	60	56
TT/TTT/5T	65	50	60	56
TT/TTT/TTTT/5T	50	50	60	53

Table 3: Gain Level Comparison over 4 flaws

*When not applicable, the surface connected crack inspected in TT is detected. The actual size is overestimated because the flaw is near to the critical refracted angle ROI. Therefore, the image is not a correct representation.

**The probe orientation and the weld bevel are always on the same side.

In general, imaging patterns with longer ultrasonic paths require more scanning gain for the same zone of interest. For those TFMi^{TM} scans incorporating a longer time of flight sound path, loss of sensitivity has been compensated by a hardware and numeric scanning gain. The scanning **Gain** parameter comes from the acquisition pipeline and **Image Sensitivity Level** is the digital image gain compensation. In all cases, the noise level of table X scan is always less than 1% full-screen height.

Regarding the mid-wall lack of fusion, it has a fairly large planar shape. The TFM works well when the scan is performed on the same side of the defect V. On the other side, when the probe is targeting 180 degrees away from the V-Weld, there is no possible echo that comes back to the probe using common classical propagation modes.

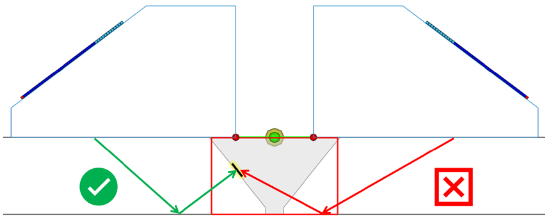

Figure 3: Mid-Wall Lack of Fusion - V-Weld

The TFMi™ inspections with the existing and proposed modes cannot resolve lack of fusion on one side scan plan. Further study on new TFMi™ modes and algorithms could possible resolve one-sided scan plan challenges where a single probe is used.

3.2 Height Sizing

The height of a defect is an important assessment property. It is used in the PA in lieu of RT (Radiography Testing) procedures[8]. In reference to annex A, we determined the vertical size by subtracting the maximum depth location of the defect minus the minimum depth. We have added the TOFD as a comparison result since this technique is a typical source of reliable height measurements[9]. Especially in this case, the 15 MHz TOFD probe creates a very short wavelength signal. We measured 0.3 mm (0.01 inch) of wavelength; Therefore, its precision is about 0.15 mm considering that wave should contain at least 4 samples (acquisition rate at 200 MHz).

There is a preferred mode among the shear wave TFM mode in every case. The best mode is the one that has the lowest beam width, best sensitivity and best SNR. The table of results is in the Annex A.

The TFMi™ height assessment has a standard deviation of 0.83 mm in regards of TOFD evaluation. On the other hand, the preferred single TFM mode is 1.0 mm. By using the same setup, the intermode assessment has 17% less variation than conventional TFM scans for the same probe.

3.3 Signal to Noise Level Results

The signal-to-noise (SNR) analysis is a basic metrics to describe the quality of the image. To compare the TFMi™ scan SNR, single TFM modes have been recorded in synchronous sequences. The same setup as in Section 3.1 has been used. The results below are the center-line crack result. Higher SNR means the better a result as shown in the following formula:

$$SNR = 20 \log \left[\frac{Peak_{Mode}}{Baseline\ \ noise} \right]$$

TT	TTT	TTTT	TT/TTT/TTTT
22 dB	11 dB	10 dB	44 dB

The multiplication of the baseline noise pixel decreases considerably. During the TFMi™ acquisition pipeline, there is no amplitude amplification when all the mode samples are near the zero baseline. The multiplicative Intermode algorithm is in fact approximating the behaviour of the geometric mean filter[10] which is typically used in imaging applications.

The image is very clean , so a too low scanning gain is not a major issue in post-analysis. For example, in the above example, the scanning gain can still be increased by 24 dB to get a noise level of 20%FSH.

3.4 Sharpness Advantage

The multiplicative TFMi™ generates a sharp image contour during the flaw investigation. To have real metrics and a comparison with normal TFM, the slope of the indication has been calculated. The derivative has shown a 400 to 500 % per mm slope on the edge of the flaws. When we compared the same reflector in TT or TTTT, the flanks is in the 200 to 400% per mm sharpness range.

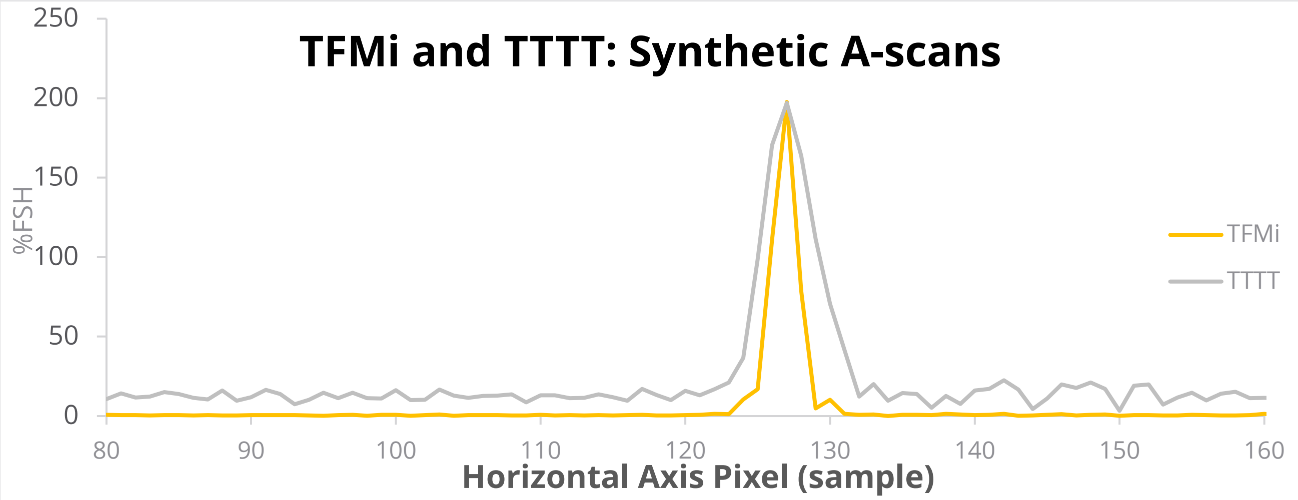

The horizontal echo width at -6 dB is 0.28 mm and 0.45 mm in the TTTT single mode. That represents a 38 % improvement. Technically, the echo should be as narrow as possible to distinguish two potential indications. Therefore, a short echo width is an important criterion for high-resolution scans. It is also a factor of improvement regarding the height assessment seen in Section 3.2.

3.5 New Considerations

3.5.1 Calibration Block Reflectors

3.5.1.1 SDH Reflector

The SDH has a volumetric and round shape. When using only 2 modes, the TT image reflects its upper hole and the TTTT reaches the bottom section of the SDH. As a matter of a fact, it is not necessarily simpler to mix the TT and TTTT on a 2 mm SDH for example. Once combined, the location of the 2 echoes is too far to show the real size of the hole. Only a small portion of the beam is creating a 0.28 mm high echo. While combining TT/TTT/TTTT though, the profile of the hole appears from the 3 reflected modes.

In all cases, TFMi™ on SDH's has not shown an absence of detection but some TFMi™ modes may enhance the shape coherence.

Table 4: Image comparison and -6 dB height evaluation; TT, TTTT, TT/TTTT and TT/TTT/TTTT over a 2 mm

TT	TTTT	TT/TTTT TFMi™	TT/TTT/TTTT TFMi™
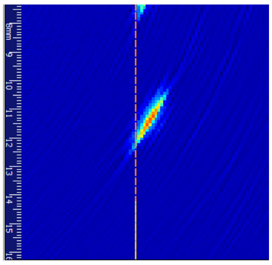	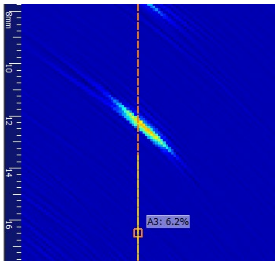	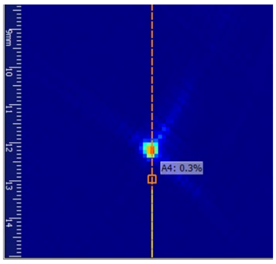	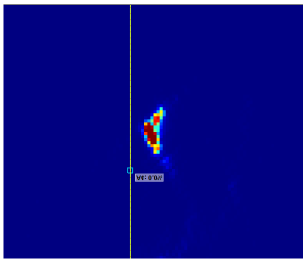
Height$_{-6dB}$ = 1.2 mm	Height$_{-6dB}$ = 0.92 mm	Height$_{-6dB}$ = 0.28 mm	Height$_{-6dB}$ = 1.61 mm

3.5.1.2 Radius Reflector

In this case the radius provides a perfect back and forth reflection. The only mode working with this reflector is the TT mode. All the other modes simply do not propagate like this. The radius is thus not a good calibration standard for the TFMi™ technique.

3.5.2 Calibrations

3.5.2.1 Reference Gain & Scanning Gain

There is not much difference to calibrate the scanning gain of an entire TFMi™ setup. The reference gain can be set to 80% FSH and to an artificial reflector. This is common in most inspections, and it is not different from the Intermode scans. All the TFM family scan are likely none-amplitude based and the ASME standard does not necessarily rely on the vertical linearity as described in EN-16392-3 for example. Here is what EN states once compared to the TFMi™ linearity. For its main purpose, the TFM is creating the best spatial indication image. When considering this side effect, the nonlinear consequence is not annoying.

2T/4T/5T Scanning Gain (relative dB)	Targeted Amplitude (%FSH)	TFMi™ *Results (%FSH) on SDH*	Acceptable Amplitude (%FSH)
+2	101	*157*	95
0	80	*80*	Reference line
-6	40	*9.3*	37 to 43
-12	20	*1.1*	17 to 23

Table 5: Amplitude PA Signal Linearity

For an automatic gain control, such as an "AUTO FULL SCREEN HEIGHT" button, the expected gain result does not work. Instead, the user must change the gain value just like any *brightness*[11] correction. It does not need to be proportional to an absolute numerical value.

Therefore, the TFMi™ scan software gain is similar to the picture corrections presented in most common editing PC software. The presented figure below illustrates the effect of gain that behaves like a brightness adjustment. The TFMi™ scanning gain is then as effective as a colour edition.

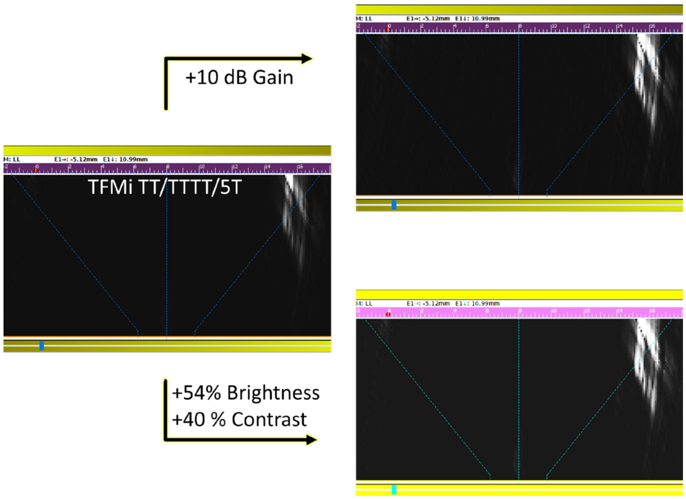

3.5.2.2 *Velocity, Probe Zero and Thickness*

As shown in Table 3, it is possible to record narrow-sized reflectors. However, doing so requires a precise calibration as the Intermode correlations must occur in the same spatial location. The geometry of the thickness is also important. An incorrect zero or thickness parameter will result in a faulty scan plan. This would prove particularly problematic for those propagation modes assuming a backwall reflection on the pulse or returning wavefront. In these cases, the image quality would be negatively affected. The strength of each calibrated TFM echo must contribute to an accurate TFMi™ image. The TFMi™ probe zero and velocity parameters must therefore be the same as a single propagation mode TFM.

3.5.2.3 *Amplitude Correction*

No exhaustive tests were made to identify the amplitude deviation in the depth axis. Luckily though, the scanning and the software gain demonstrate a low level of pixel attenuation in the scan. Vertical reflectors are consistent with each other, which gives us reason to believe that time-corrected-gain may also not be required for this type of scan. The sensitivity regions for each sub-mode compensates each other once combined. There is a sensitivity change over the type of defects and the locations and the TFMi™ could reduce the mode influence over the same scan ROI[12].

4 Conclusion

The new TFMi™ scan has demonstrated superior results on all weld flaws analyses. It outperformed competing inspection modalities with respect to SNR, height sizing and geometric flaw shape accuracy. The ability to characterise the type of defects and determine a precise height dimension is critical in pressure vessels. By adding such advanced TFM tools, the phased array level 3's could enhance the final non-destructive result. In terms of weld inspection, that is a big step forward to decrease the risk of a misinterpreted flaw.

For advanced PAUT inspectors and all NDT researchers, it also advances automatic flaw recognition over the TFMi™ scans and gives greater precision for critical inspections.

5 Annex A

Weld Flaw	**TT** TFM (mm)	**TTT** or **5T** TFM (mm)	**TT-TT** TFM (mm)	**TFMi™** Evaluation (mm)	**TOFD** (mm)	Flawtech UT Assessment (± 3.8 mm)
UT-3546-Root crack in single V	5.6	4	Invisible	5.4	5.0	3.8
UT-3546-Slag inclusion in root	5.5	5.9	5.6	5.0	5.15	5.0
UT-3549-Base metal crack (top HAZ)	Invisible	6.4	6.3	6.4	7.2	3.8
UT-3549-Base metal crack (bottom HAZ)	5.6	4.6	4.6	4.65	3.4	3.8
UT-3544-Center line crack sub-surface	4.1	3.1	3.5	4.0	4.6	3.8
UT-3544-Porosity in single V sub-surface	Near Invisible	Near Invisible	4.9	4.5	4.5	3.8
UT-3547- Lack fusion mid-wall V	Invisible	Invisible	3.25	3.0	4.08	3.8
UT-3547- Lack of fusion root	4.1	6.2	3.5 (diffraction echo)	4.5	5.72	3.8

Preferred TFM Mode

*All TFM scans are recorded with 7.5 MHz, 44 Element, 0.6 mm pitch Phased array probe. TFMi™ scans were set to 2T-4T-5T or 2T-3T-4T. The TOFD scans were at 15 Mhz.

---

[1] **BS ISO 23864:2021** Non-destructive testing of welds — Ultrasonic testing — Use of automated total focusing technique (TFM) and related technologies. Section 4.

[2] **American Society of Mechanical Engineers.** Section V, Article 4, Imaging modes section in Mandatory Appendix F. XI481.1.1

[3] **Jeremy CARIGNAN, Marie-Pierre DESPAUX, François LACHANCE, Philippe RIOUX,** *Sensitivity Response of Total Focusing Method (TFM) for Weld Inspection Versus Other Techniques.* Canada: Centre de métallurgie du Québec, Sonatest AP, Québec, 2019.

[4] **Xiaoli HAN, Wentao WU, Di ZHANG, Haitao WAN**. Combination of direct, half-skip and full-skip TFM to characterize defect (2). Beijing, China: Chinese Academy of Sciences, 2019.

[5] **Rhodri L.T. BEVAN.** *Data fusion of multi-view ultrasonic imaging for characterisation of large defects*. United Kingdom: University of Bristol. 2020.

[6] **American Society of Mechanical Engineers.** Section V, Article 4, Imaging modes section in Mandatory Appendix F.

[7] **Jeremy CARIGNAN, Marie-Pierre DESPAUX, François LACHANCE, Philippe RIOUX,** *Sensitivity Response of Total Focusing Method (TFM) for Weld Inspection Versus Other Techniques.*

[8] **American Society of Mechanical Engineers.** Section V, Article 4 and 7.5.5, Ultrasonic examination (when used in lieu of RT).

[9] **Towards an Alternative to Time of Flight Diffraction Using Instantaneous Phase Coherence Imaging for Characterization of Crack-Like Defects.** Baptise GAUTHIER, Guillaume PAINCHAUD APRIL, Alain le Duff and Pierre BÉLANGER. Hyunjo Jeong, 22 January 2021

[10] https://en.wikipedia.org/wiki/Geometric_mean_filter, Geometric mean filter, Wikipedia.

[11] https://en.wikipedia.org/wiki/Brightness Brightness, Wikipedia web page.

[12] **Sy, Kombossé.** *Étude du développement de méthodes de caractérisation de défauts basée sur les reconstructions ultrasonores TFM.* Paris : Université Paris-Saclay, 2018.